Biochimica et Biophysica Acta 1847 (2015) 1075–1084

Contents lists available at ScienceDirect

Biochimica et Biophysica Acta

journal homepage: www.elsevier.com/locate/bbabio

Disruption of cytochrome *c* heme coordination is responsible for mitochondrial injury during ischemia

Alexander V. Birk, Wesley M. Chao, Shaoyi Liu, Yi Soong, Hazel H. Szeto *

Department of Pharmacology, Joan and Sanford I. Weill Medical College of Cornell University, New York, NY 10065, USA
Research Program in Mitochondrial Therapeutics, Joan and Sanford I. Weill Medical College of Cornell University, New York, NY 10065, USA

ARTICLE INFO

Article history:
Received 10 April 2015
Received in revised form 13 May 2015
Accepted 7 June 2015
Available online 10 June 2015

Keywords:
Methionine sulfoxide
cyt *c* oxygenase
Electron transport
SS-20
OPA1
Mitochondria cristae

ABSTRACT

Background: It was recently suggested that electron flow into cyt *c*, coupled with ROS generation, oxidizes cyt *c* Met^{80} to Met^{80} sulfoxide (Met-O) in isolated hearts after ischemia–reperfusion, and converts cyt *c* to a peroxidase. We hypothesize that ischemia disrupts Met^{80}-Fe ligation of cyt *c*, forming pentacoordinated heme Fe^{2+}, which inhibits electron transport (ET) and promotes oxygenase activity.
Methods: SS-20 (Phe-D-Arg-Phe-Lys-NH_2) was used to demonstrate the role of Met^{80}-Fe ligation in ischemia. Mitochondria were isolated from ischemic rat kidneys to determine sites of respiratory inhibition. Mitochondrial cyt *c* and cyt *c* Met-O were quantified by western blot, and cristae architecture was examined by electron microscopy.
Results: Biochemical and structural studies showed that SS-20 selectively targets cardiolipin (CL) and protects Met^{80}-Fe ligation in cyt *c*. Ischemic mitochondria showed 17-fold increase in Met-O cyt *c*, and dramatic cristaeolysis. Loss of cyt *c* was associated with proteolytic degradation of OPA1. Ischemia significantly inhibited ET initiated by direct reduction of cyt *c* and coupled respiration. All changes were prevented by SS-20.
Conclusion: Our results show that ischemia disrupts the Met^{80}-Fe ligation of cyt *c* resulting in the formation of a globin-like pentacoordinated heme Fe^{2+} that inhibits ET, and converts cyt *c* into an oxygenase to cause CL peroxidation and proteolytic degradation of OPA1, resulting in cyt *c* release.
General significance: Cyt *c* heme structure represents a novel target for minimizing ischemic injury. SS-20, which we show to selectively target CL and protect the Met^{80}-Fe ligation, minimizes ischemic injury and promotes ATP recovery.

1. Introduction

Mitochondria play a crucial role in cellular energy generation and must respond to ever-changing metabolic challenges to meet cellular energy demands. Under ischemic conditions, the deficiency of substrates and oxygen inhibits mitochondrial respiration and prevents ATP production. There is a rapid fall in tissue ATP content as a result of decreased ATP production, reversal of the ATP synthase to hydrolyze ATP, and continuous cellular energy expenditure. Timely reperfusion is the only means to reduce necrotic cell death and prevent organ failure. However, reperfusion does not result in full recovery of ATP content [1,2]. Although much attention has been given to reperfusion injury caused by the rapid release of reactive oxygen species (ROS) from ischemic mitochondria, other studies suggest that ischemia itself causes permanent injury to the mitochondrial electron transport chain (ETC) [1,3,4]. Studies using mitochondria isolated from ischemic tissues have shown significant decreases in coupled respiration and increased electron leak at complexes I and III, suggesting an obstruction of electron transport (ET) downstream of complex III, either at cytochrome (cyt) *c* or complex IV [1,4–6]. The inhibition of complex IV (also known as cytochrome *c* oxidase, COX) activity does not appear to result from functional inactivation of the protein complex, but has been suggested to be secondary to the loss of cardiolipin (CL) and cyt *c* [6–9].

Cyt *c* is the only component of the ETC that is not embedded in the inner mitochondrial membrane (IMM). Cyt *c* mediates ET *via* reduction and oxidation of its hexacoordinated heme iron (Fe) that is stabilized by the axial ligands Met^{80} and His^{18} [10–12]. Electrostatic interaction between cyt *c* and CL anchors cyt *c* to the IMM and optimizes ET between complex III and complex IV [13]. Interestingly, low ATP conditions favor hydrophobic interaction between cyt *c* and CL [14,15], which is known to disrupt the Met^{80}-Fe ligation, resulting in a pentacoordinated heme Fe [16–19]. The loss of the Met^{80}-Fe ligation inhibits ET and converts cyt *c* from an electron carrier to an oxygenase/peroxidase that can cause CL peroxidation [12,20–23]. However, most of these studies were done in cell-free *in vitro* systems, and the biological relevance of this pentacoordinated cyt *c* is unclear. We hypothesize that ATP

* Corresponding author at: Department of Pharmacology, Weill Cornell Medical College, 1300 York Avenue, New York, NY, USA.
E-mail address: hhszeto@med.cornell.edu (H.H. Szeto).

http://dx.doi.org/10.1016/j.bbabio.2015.06.006
0005-2728/

deficiency during ischemia disrupts cyt *c* heme ligation, and the pentacoordinated heme Fe^{2+} accounts for inhibition of ET and CL peroxidation during ischemia.

Recent studies showed increase in oxidation of Met^{80} to the Met^{80}-sulfoxide (Met^{80}-O), and loss of cardiolipin in the ischemic isolated hearts after 30 min of reperfusion [24]. Since Met^{80} can only undergo self-oxidation when it is not coordinating the heme Fe [19], these results support *ex vivo* formation of pentacoordinated cyt *c* during ischemia–reperfusion. Using normal isolated mitochondria, these investigators proposed that electron flow through cyt *c*, coupled with excessive ROS production, is required for the oxidation of Met^{80} [24]. However, the conditions required for cyt *c* Met-O formation and ROS formation in isolated mitochondria are not the same [24], so it remains uncertain whether inhibition of ET or excessive ROS, or both required for Met-O formation and peroxidase activity.

Using an *in vivo* model of renal ischemia, we found significant inhibition of mitochondrial respiration and cristeolysis during ischemia alone [25,26]. Administration of SS-31, a mitochondria-targeted antioxidant [27], protected cristae structure during ischemia, and greatly accelerated ATP recovery upon reperfusion [25]. Although we subsequently demonstrated that SS-31 inhibits peroxidase activity of pentacoordinated cyt c *in vitro* [26], it is not clear whether this was due to its antioxidant properties [27,28] or its ability to protect the cyt *c* heme environment [26]. To resolve this issue, we decided to use another mitochondria-targeted peptide, SS-20, which does not scavenge ROS [27,28], to investigate the *in vivo* implications of pentacoordinated cyt *c*. Similar to SS-31, SS-20 was found to protect cristae architecture, prevent cyt *c* loss, promote recovery mitochondrial respiration upon reperfusion, and preserve organ function [2], indicating the importance of pentacoordinated cyt *c* in ischemic injury. We also found increased Met-O cyt *c* formation during renal ischemia, which was prevented by SS-20, lending support for the formation of pentacoordinated cyt *c* *in vivo*. In addition, we show that SS-20 prevents degradation of OPA1 (Optic Atrophy 1), an essential IMS protein for maintenance of cristae junctions on the IMM and prevention of cyt *c* release [29–31], thereby suggesting that cyt *c* peroxidase activity might initiate catalytic degradation chain reaction on the IMM.

2. Materials and methods

2.1. Chemicals

Phe-D-Arg-Phe-Lys-NH_2 (SS-20) was provided by Stealth Peptides Inc., Newton Centre, MA. Aladan (ald; 2-amino-4-(6-(dimethylamino)naphthalen-2-yl)-4-oxobutanoic acid) was synthesized by J. David Warren (Weill Cornell Medical College) from commercially available 6-methoxy-2-acetonaphthone, as described in our recent publications [13,26]. Phe-D-Arg-Ald-Lys-NH_2 ([ald]SS-20) was synthesized by Dalton Pharma Services (Toronto, Ontario, Canada). 1-palmitoyl-2-oleoyl-*sn*-glycero-3-phosphocholine (POPC), 1,2-dihexanoyl-sn-glycero-3-phosphocholine (DHPC), and natural CL from bovine heart (containing 90% 18:2 acyl chains) were obtained from Avanti Polar Lipids Inc. (Alabaster, AL). Horse heart cyt *c* and all other reagents were obtained from Sigma-Aldrich, (St. Louis, MO).

2.2. Animals

Adult male Sprague–Dawley rats (Charles River Laboratories International, Inc., Wilmington, MA) weighing 250 to 300 g were used in the study. Animals were housed in a light-controlled room with a 12:12-hour light-dark cycle and allowed free access to water and standard rat chow. Care of the rats before and during the experimental procedures was conducted in accordance with the policies of the National Institutes of Health Guidelines for the Care and Use of Laboratory Animals. All protocols had received prior approval by the Cornell University Institutional Animal Care and Use Committee.

2.3. Rat model of renal ischemia–reperfusion injury

Adult male Sprague–Dawley rats (250 to 300 g) were anesthetized with 90 mg/kg ketamine and 4 mg/kg xylazine. Bilateral renal ischemia was induced by the application of nontraumatic microvascular clamps around both left and right renal pedicles for 45 min, as described in detail previously [25,26]. Sham-operated animals were not subjected to ischemia. Animals were randomly assigned to the following groups: sham-operated, ischemia with saline, or ischemia with SS-20. SS-20 (2 mg/kg) or saline was administered subcutaneously 30 min before the onset of ischemia. Animals were sacrificed and kidneys harvested right after ischemia.

2.4. Preparation of rat kidney mitochondria and mitoplasts

Mitochondria were isolated from normal rat kidneys or ischemic kidneys as described previously [13]. Mitochondria were either used immediately for respiration experiments or frozen at −80 °C until time of use for experiments with once-frozen mitochondria. The integrity of freshly isolated mitochondria was demonstrated by observing no effect of exogenously added 20 μM cyt *c* on mitochondrial respiration. To prepare mitoplasts, the outer membranes of fresh or once-frozen mitochondria were removed by 45 minute exposure to 3.3 mg/ml digitonin on ice [13]. To remove electrostatically-bound cyt *c*, 300 mM KCl was added and the mixture was centrifuged for 30 min at 14,000 ×*g*. The supernatant was discarded, and the pellet was washed with 300 mM KCl and re-dissolved in wash buffer and stored on ice until use. Only those mitoplast preparations that show an increase in mitochondrial respiration by 4-6 fold upon addition of 400 nM of exogenous house heart cyt *c* were used.

2.5. Oxygen consumption

Oxygen consumption in freshly isolated mitochondria was measured as described previously [13,26]. 40 μg/ml of freshly isolated mitochondria from normal animals was incubated with 400 μM ADP (state 2) at 37 °C for 1 min, then succinate (500 μM) (complex II substrate) or glutamate/malate (500 μM each) (complex I substrates) was added to initiate state 3 respiration. TMPD (N,N,N′,N′-tetramethyl-p-phenylenediamine) (3 μM)/ascorbate (500 μM) system was used to directly reduce cyt *c* in intact mitochondria. Mitochondrial respiration was allowed to proceed to state 4. SS-20 was added to the mitochondria prior to onset of respiration studies. Mitochondria isolated from Sham, ischemia, or ischemia/SS-20 animals were also subjected to the same treatment but respiration was studied without addition of SS-20. Since the rate of oxygen consumption in general state 3 consists of ATP synthase-driven respiration (OXPHOS-driven) and nonspecific proton leak-driven respiration (state 4), the final state 3 (OXPHOS-driven respiration) was calculated as the difference between general state 3 and state 4. Respiratory control ratio was calculated as a ratio of general state 3 to state 4.

Oxygen consumption in once-frozen mitochondria directly indicates ET through mitochondrial respiratory complexes because once-frozen mitochondria have permeable outer and inner mitochondrial membrane and thereby, have no mitochondrial membrane potential. Succinate (500 μM) was used to measure ET from complex II to complex IV. TMPD (3 μM)/ascorbate (500 μM) was used to directly reduce cyt *c* and initiate ET to COX.

Oxygen consumption in cyt *c*-deficient mitoplasts was measured with 40 μg of mitoplast in 1 ml of 20 mM Hepes buffer, pH 7.4, after initiating respiration with TMPD (250 μM)/ascorbate (5 mM) in the presence of antimycin (2 μM) to block complex III. SS-20 was added to the mitoplasts before initiating respiration. After the initial low respiration in mitoplasts, exogenous horse heart cyt *c* (400 nM) alone was added to promote respiration. Alternatively, 60 μM CL was also added together with cyt *c* to block respiration through cyt *c*.

2.6. COX activity

To measure COX activity in cyt *c*-deficient mitoplasts from sham, ischemia, or ischemia/SS-20 animals, 10 μg of mitochondria was mixed with 20 μM maximally reduced cyt *c* (with 20 μM ascorbate) and oxidation of cyt *c* was measured at 550 nm with reference wavelength at 570 nm. The reaction was done in respiration buffer [13] at room temperature for 15 s.

2.7. Mitochondrial membrane potential

Mitochondrial potential was qualitatively assessed by measuring quenching of TMRM fluorescence signal (excitation/emission = 550/575 nm) [32]. The fluorescence of this lipophilic cation is quenched when it is taken up by mitochondria, and restored when mitochondria become depolarized. In brief, isolated mitochondria (0.3 mg) were added to 2.0 ml of buffer (70 mm sucrose, 230 mm mannitol, 3 mm HEPES, 2 mm Tris-phosphate, 5 mm succinate, and 1 μm rotenone) containing TMRM (0.4–2 μm). Mitochondrial potential was quantified by quenching of the fluorescent signal [27,33].

2.8. Western blot assays for cyt c, Met-O cyt c, and OPA1

Frozen mitochondria were homogenized and sonicated and then added to RIPA buffer (Santa Cruz, Santa Cruz, CA). Homogenates (10 μg) were suspended in loading buffer and subjected to a 4–15% SDS-PAGE precast gel (Bio-Rad, Hercules, CA) electrophoresis. The resolved proteins were transferred to a PVDF membrane. For detecting Met-O after electroblotting, membranes were incubated overnight with anti-methionine sulfoxide (Abcam, Cambridge, MA), rabbit polyclonal IgG 1:500 in 5% milk/TBST) and then with secondary goat anti-rabbit IgG-HRP (Vector, Burlingame, CA) (1:5000 in 5% milk) for 1 h. For cyt *c* detection, the same membranes were stripped and incubated for 2 h with anti-cyt *c* mouse monoclonal IgG (Abcam, Cambridge, MA) and another hour with HRP-conjugated monoclonal goat anti-mouse IgG (Dako, Carpinteria, CA). OPA1 was detected by overnight incubation with anti-OPA1 rabbit polyclonal IgG (Abcam, Cambridge, MA) 1:1000 in 5% milk followed by one hour incubation with secondary goat anti-rabbit IgG-HRP 1:5000 in 5% milk (Vector, Burlingame, CA). All protein bands were detected by chemiluminescence with Clarity™ Western ECL Substrate (Bio-Rad, Hercules, CA) and autoradiography. Bands were evaluated for integrated density values using Image Lab™ Software (Bio-Rad, Hercules, CA). All membranes were finally stained with Coomassie blue to determine the amount of protein for normalization of cyt *c* in each lane.

2.9. Preparation of liposomes and bicelles

Lipids in chloroform were combined in 12 × 75 mm glass tubes in the ratios for forming liposomes and bicelles, as described previously [13]. Liposomes contained either 150 μM CL: 150 μM POPC or 300 μM POPC. Bicelles contained either 150 μM CL: 1500 μM POPC: 4500 μM DHPC or 1500 μM POPC: 4500 μM DHPC. The solvent was evaporated slowly under N_2 gas (TechAir, Naugatuck, CT, USA), and the resulting lipid film was rehydrated in an aqueous solution of 20 mM HEPES pH 7.4 or deuterated water (D_2O) buffered with 5 mM Na_2PO_4 and titrated with HCL to a final pH of 6.5 (for NMR studies). The resulting multilamellar vesicles were vortexed lightly, and sized into small unilamellar vesicles by 25 min of heated bath sonication (Solid State Ultrasonic FS-9, 40 kHz, Fischer Scientific). Bicelles were not sonicated. All liposomes and bicelles were cooled to ambient temperature before use.

2.10. Interaction of [ald]SS-20 and SS-20 with CL

To investigate if SS-20 interacts with CL, we incorporated a polarity-sensitive fluoroprobe (aladan) into SS-20 [13] (Supplementary Fig. 1). The fluorescence emission spectrum of aladan (λex = 360 nm) was obtained with 2 μM [ald]SS-20 in H_2O, or after the addition of 10 μM POPC or POPC:CL (SPECTRAmax GeminiXPS, Molecular Devices, Sunnyvale, CA). The interaction of SS-20 with CL was confirmed by measurement of changes in turbidity caused by the formation of a peptide-CL complex *via* right-angle scattering at λ = 350 nm (Hitachi F-4500 Fluorescent Spectrophotometer).

2.11. NMR analysis of SS-20 and CL interaction

NMR experiments were collected on a Bruker Avance III 500 MHz NMR spectrometer equipped with a 5 mm broad-band with z-gradient pulse field gradients. The variable temperature unit was calibrated using a thermocouple placed inside a filled NMR tube within the probe. The chemical shifts were referenced with 4,4-dimethyl-4-silapentane-1-sulfonic acid (DSS) as an internal reference. Chemical shifts of aromatic amino acids in SS peptides were previously characterized [13]. NMR SS-20-lipid binding experiments were carried out using bicelles containing either 150 μM TOCL: 1500 μM POPC: 4500 μM DHPC or 1500 μM POPC: 4500 μM DHPC in 5 mM sodium phosphate adjusted to pH 6.5 (uncorrected for isotope shifts) using ^2HCl. Bicelles are small lipid bilayers that form disk-like particles in solution. They are composed of long chain lipids, which form a planar surface surrounded by short chain lipids coating the edges. The small size of these bicelles allows proteins/peptides to be analyzed by solution NMR, providing good spectral characteristics (~21 kDa for POPC/DHPC q = 0.15 to 0.3) [13,34]. POPC/DHPC bicelles have been demonstrated to best approximate biological lipids in membrane protein crystallography studies and NMR studies [13]. The proton assignment for free SS-20 was determined using 1D NMR. The phenylalanine (Phe) peak was observed between 7.4 and 7.2 ppm, in a region where POPC and CL are known to have no peaks [13]. NMR data were processed and analyzed using Topspin 2.1 (Bruker Corporation) and MestReNova (Mestrelab Research S.L., Santiago de Compostela, Spain).

2.12. Interaction of [ald]SS-20 with cyt c-deficient mitoplasts, mitochondria, purified cyt c, and cyt c in the presence of CL

To determine if SS-20 can interact with endogenous CL in mitochondria, we measured the fluorescence emission spectra of [ald]SS-20 after addition of mitoplasts or frozen mitochondria (~40 μg/ml). To determine if [ald]SS-20 interacts with cyt *c* in the presence of CL, 2 μM [ald]SS-20 was added to a mixture of 2 μM cyt *c* and 10 μM POPC:CL liposomes. The interaction between [ald]SS-20 and cyt *c* alone was included to see if the peptide would interact directly with cyt *c* in the absence of CL. The fluorescence emission spectrum of [ald]SS-20 (λex = 360 nm) was obtained using the SPECTRAmax GeminiXPS (Molecular Devices, Sunnyvale, CA).

2.13. Interaction of SS-20 with cyt c in the presence of CL

The interaction of SS-20 with cyt *c* in the presence of CL was examined by circular dichroism performed with an AVIA 62 DS spectrophotometer equipped with a sample temperature controller. The CD spectrum of the Soret region (370–450 nm) was recorded with 10-mm path length cells containing 20 mM Hepes, pH 7.4, and 10 μM cyt *c*, in the presence or absence of 30 μg/ml CL and 10 μM SS-20. The maximum lipid concentration was kept low to avoid spectral distortions due to excessive light scattering. All measurements were done at 25 °C. All spectra were corrected for background, and the final spectrum shown represents the average of at least three experiments.

2.14. Peroxidase activity of cyt c in the presence of CL

The effect of SS-20 on CL-induced cyt *c* oxygenase/peroxidase activity was determined using the Amplex Red assay without the addition of

horseradish peroxidase [13]. Cyt *c* (2 μM) was incubated with CL (30 μM) for 1 min in 200 μl HEPES (pH 7.5) in the absence or presence of 10 μM H_2O_2 and 50 μM Amplex Red reagent, and the reaction was allowed to proceed for an additional 5 min. For some experiments 1 mM CaCl was incubated together with cyt *c* and CL prior to the addition of 10 μM H_2O_2 and 50 μM Amplex Red reagent, to investigate effects of calcium on peroxidase activity. The continuous time course data were obtained using a microplate spectrofluorometer (Molecular Devices, Sunnyvale, CA).

2.15. Cyt c reduction and electron transport in the presence of CL

Cardiolipin is known to inhibit the reduction of cyt *c* [13–15]. Cyt *c* (20 μM) was preincubated with CL, in the absence or presence of different concentrations of SS-20, for 1 min. Cyt *c* reduction was initiated by the addition of 500 μM glutathione. The rate of cyt *c* reduction was calculated from the slope of (A_{550}–A_{570}) over 2 min (SPECTRAmax 190, Molecular Devices, Sunnyvale, CA). The ability of SS-20 to promote electron transfer in the ETC was determined by measurement of oxygen consumption in mitoplasts (Hansatech Instruments, Norfolk, UK) [13]. Respiration was initiated in mitoplasts (40 mg) with TMPD (250 μM)/ascorbate (5 mM). Antimycin (2 μM) was added to block complex III. As these mitoplasts are deficient in cyt *c*, exogenous cyt *c* (400 nM) was added to promote respiration.

2.16. H_2O_2 release in mitochondria

The rate of mitochondrial H_2O_2 generation was determined in separate experiments where mitochondria were incubated with succinate (5 mM) and no ADP for 15 min. The reaction was stopped and centrifuged at 14,000 ×*g*, 4 °C, for 5 min. The supernatant was collected and the amount of H_2O_2 released determined using the Amplex Red assay (λex/λem = 570/585 nm).

2.17. Electron microscopy

Kidney tissues were fixed in 4% paraformaldehyde, postfixed in 1% osmium tetroxide, dehydrated in graded alcohols, and embedded in Epon. Ultrathin sections (200 to 400 Å) were cut on nickel grids, stained with uranyl acetate and lead citrate, and examined using a digital electron microscope with a 2.0 CCD camera (JEOL USA JEM-1400, Peabody, MA).

2.18. Statistical analysis

All results are expressed as mean ± SEM. Statistical analyses were carried out using one-way ANOVA analysis with multiple comparisons or *t*-test (GraphPad Software, Inc., San Diego, CA).

3. Results

3.1. SS-20 preserves mitochondrial ET through cyt c in ischemic mitochondria

To determine the effect of ischemia on mitochondrial respiration upon reperfusion, we isolated kidney mitochondria from rats after 45 min ischemia. Mitochondrial respiratory activity was initiated from different respiratory complexes *ex vivo*. State 3 respiration (coupled to ATP synthesis) was significantly inhibited in ischemic mitochondria induced by complex I substrates (Fig. 1A) or complex II substrates (Fig. 1B) compared to sham controls. In contrast, state 4 respiration (uncoupled from OXPHOS) was unchanged (Fig. 1C and D), suggesting that in contrast to mitochondria isolated after reperfusion [4], proton leak is not increased in ischemic mitochondria. Ischemia significantly reduces O_2 consumption induced by direct reduction of cyt *c* with N,N,N,N-tetramethyl-p-phenylenediamine (TMPD) (Fig. 1E) without altering COX activity (Fig. 1F), indicating that cyt *c* is the site of ET inhibition during ischemia. Importantly, ischemic mitochondria from the SS-20 treated group demonstrated considerable improvement of ET function, with significant improvement in state 3 respiration. There was no effect on state 4 respiration, showing that SS-20 does not uncouple mitochondrial respiration (Fig. 1A–D). TMPD-induced respiration was also protected in SS-20-treated animals, without increasing the activity of COX (Fig. 1E and F), suggesting that SS-20 selectively targets cyt *c* and prevents ET dysfunction during ischemia.

3.2. SS-20 prevents oxidative modification of cyt c and cyt c release during ischemia

Mitochondria from sham animals revealed very low Met-O cyt *c* formation, while 45 min ischemia alone induced a 17-fold increase in Met-O cyt *c* (Fig. 2A). Treatment with SS-20 significantly reduced Met-O cyt *c* formation (Fig. 2A). Increase in Met-O cyt *c* formation correlated well with cyt *c* release from mitochondria and SS-20 completely prevented the loss of mitochondrial cyt *c* (Fig. 2B).

3.3. SS-20 prevents cristaeolysis and degradation of OPA1 during ischemia

To better understand how cyt *c* is released from mitochondria during ischemia, we examined mitochondrial structure using transmission electron microscopy. We focused on mitochondria in the proximal tubules because they rely solely on mitochondria for ATP synthesis as they lack glycolytic capability [35–37]. In sham samples, mitochondria were elongated with densely-packed cristae membranes (Fig. 2C). 45 min of ischemia resulted in large, rounded mitochondria with matrix swelling and disappearance of cristae structures. Outer mitochondrial membranes remained mostly intact. Mitochondrial swelling was dramatically reduced by SS-20 treatment, and matrix density and cristae morphology were largely preserved.

Cyt *c* is normally sequestered in the intracristae space (ICS) due to the presence of cristae junctions on the IMM. OPA1 is a protein that is located at cristae junctions and serves to maintain cristae morphology [29–31]. Loss of OPA1 causes disorganization of cristae membranes and loss of cyt *c*. Proteolytic degradation of OPA1 is induced by dissipation of mitochondrial membrane potential and leads to loss of cristae morphology [31,38]. It is not known if ischemia will induce proteolysis of OPA1 and cause cyt *c* release. We examined the various isoforms of OPA1 using western blot. With ischemia, there was increased processing of the long-form OPA1 (~110 kDa) (L-OPA1) to lower molecular weight bands at ~100 kDa (intermediate form of OPA1, I-OPA1) and ~85 kDa (S-OPA1) (Fig. 2D). Treatment with SS-20 significantly reduced the processing of L-OPA1 (Fig. 2D and E), which also correlates with the ability of SS-20 to preserve cristae structure (Fig. 2C).

3.4. SS-20 preserves Met^{80}-Fe ligation and protects ET properties of cyt c while inhibiting peroxidase activity

The ability of SS-20 to protect ET through cyt *c* and prevent Met^{80} oxidation suggests that SS-20 might act by protecting the Met^{80}-Fe ligation during ischemia. Previous studies have shown that low ATP conditions promote hydrophobic interaction between cyt *c* and CL, which disrupts the Met^{80}-Fe ligation and results in a more open heme crevice [16,17,39,40]. The Met^{80}-Fe ligation can be monitored by circular dichroism [41]. The addition of CL to cyt *c* results in loss of the negative Cotton peak at 419 nm and this is restored by the addition of SS-20 in a 1:1 ratio with cyt *c* (Fig. 3A), providing evidence that SS-20 can protect the Met^{80}-Fe coordination in the presence of CL and preserve the closed heme crevice. Disruption of the Met^{80}-Fe bond lowers the redox potential of cyt *c* and decreases ET rate through cyt *c* [20,21]. SS-20 dose-dependently restored the ability of glutathione to reduce Fe^{3+} cyt *c* in the presence of CL, while it had no effect on native cyt *c* (Fig. 3B). In mitoplasts, addition of CL also inhibited O_2 consumption

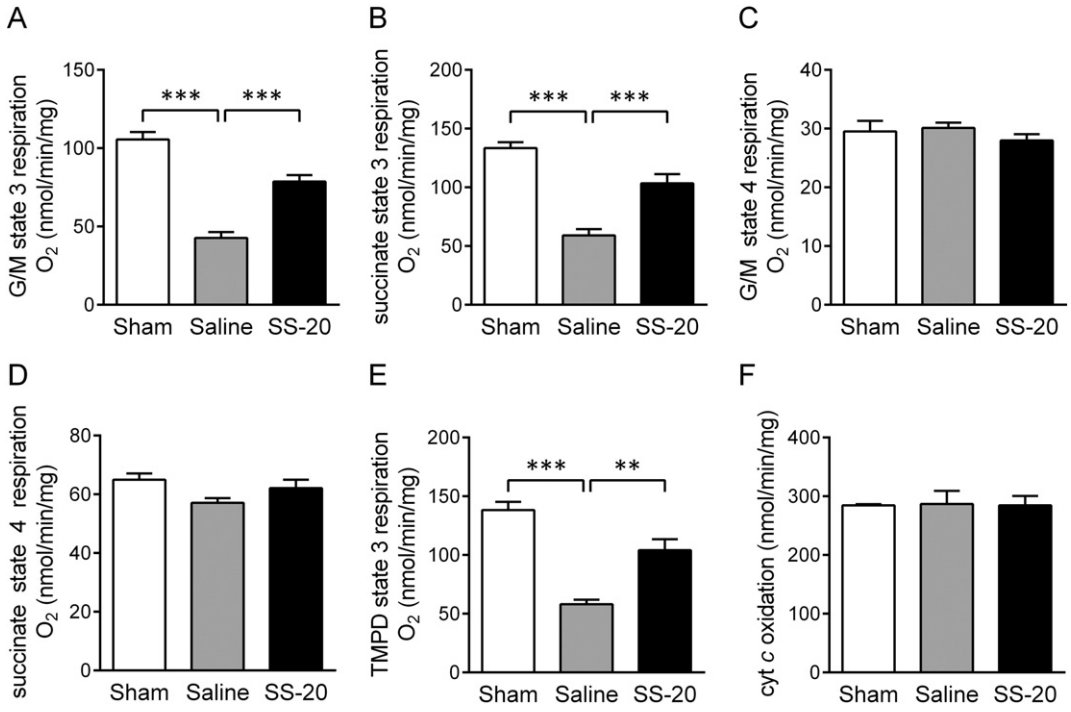

Fig. 1. SS-20 preserves mitochondrial ET through cyt *c* in ischemic mitochondria. A–B, Ischemia compromises state 3 respiration in rat kidney mitochondria when electron transport is initiated by glutamate/malate (G/M) (Complex I) (A) or succinate (Complex II) (B). SS-20 significantly restores respiration in each case. C–D, Ischemia does not change state 4 respiration in rat kidney mitochondria when initiated by complex I (C) or complex II (D) substrates. SS-20 has no effect. E, Ischemia reduces state 3 respiration initiated by direct reduction of cyt *c* using TMPD. SS-20 restores respiration. F, Ischemia does not change the ability of COX (Complex IV) in isolated mitoplasts to oxidize exogenous cyt *c*, and SS-20 has no effect. Error bars represent SEM (n = 4–10) $^{**}P = 0.01$; $^{***}P = 0.001$.

elicited by direct reduction of exogenously added cyt *c* with TMPD (Fig. 3C). Addition of SS-20 to that system significantly prevented the inhibitory action of CL on cyt *c* reduction (Fig. 3C).

Globin-like pentacoordinated cyt *c* can react with oxygen or H_2O_2 to promote oxygenase/peroxidase activity of that enzyme [22,23,26]. Calcium, which is elevated during ischemia, was recently shown to potentiate peroxidase activity of cyt *c* [26]. We determined cyt *c* oxygenase/peroxidase activity using the Amplex Red assay. Addition of CL to cyt *c* in the absence of H_2O_2 elicits oxygenase activity that is dose-dependently inhibited by SS-20 (data not shown). Addition of H_2O_2 increased the rate of the reaction, and SS-20 inhibited this peroxidase activity with similar EC_{50} (~30 μM) either in the presence or absence of calcium (Fig. 3D and E).

3.5. SS-20 binds selectively to mitochondrial CL and interacts with cyt c

To understand how SS-20 protects the heme environment of cyt *c* in the presence of CL, we synthesized a fluorescent analog of SS-20 by substituting Phe^3 with aladan (Ald), a polarity-sensitive fluorescent amino acid [42], resulting in [ald]SS-20 (H-Phe-D-Arg-Ald-Lys-NH_2) (Supplemental Fig. 1). Addition of liposomes containing POPC and CL, but not POPC alone, dramatically increases fluorescence of [ald]SS-20 and blue-shifts the λmax from 535 nm to 465 nm, demonstrating a selective hydrophobic interaction between [ald]SS-20 and CL-containing membranes (Fig. 4A). Right-angle light scattering also confirms specific interaction between SS-20 and CL, and suggests maximal interaction at an SS-20:CL molar ratio of ~2 (Fig. 4B). 1D ^{1}H NMR demonstrates specific interaction between SS-20 and bicelles containing 2.5% CL, where the side chain resonances of Phe (7.2–7.4 ppm) are suppressed (Fig. 4C), suggesting penetration of the aromatic rings into the lipid bilayer. To determine whether SS-20 can interact with endogenous CL in mitochondria, [ald]SS-20 was added to once-frozen mitochondria or cyt *c*-deficient mitoplasts, and a similar blue-shift of the λmax of [ald]SS-20 was observed (Fig. 4D). Surprisingly, the increase in fluorescence intensity of [ald]SS-20 was significantly greater with cyt *c*-depleted mitoplasts (Fig. 4D and E), suggesting that the fluorescence of [ald]SS-20 in frozen mitochondria may be partially quenched by the cyt *c* heme. To confirm this idea, we demonstrated that the fluorescence intensity of [ald]SS-20 is quenched by cyt *c* in the presence of CL (Fig. 4F), though addition of cyt *c* alone does not change the fluorescence spectrum of [ald]SS-20. Therefore, our data show that in the presence of CL, SS-20 is able to penetrate into the heme environment of cyt *c*.

3.6. SS-20 promotes efficiency of ET and inhibits ROS formation in isolated mitochondria

Low ATP conditions are known to promote hydrophobic interaction between cyt *c* and CL and inhibit cyt *c* reduction. Under conditions normally used for isolating mitochondria, mitochondrial ATP levels are very low, and this may impact measurements of mitochondrial respiration *ex vivo*. These conditions also reflect *in vivo* conditions of ischemic mitochondria subjected to reperfusion, except that cyt *c* concentrations may be normal. Addition of SS-20 to freshly isolated intact mitochondria dose-dependently increases state 3 O_2 consumption initiated from complexes I or II (Fig. 5A and C) and respiratory control ratio (RCR) (Fig. 5B and D), supporting our hypothesis that SS-20 promotes efficiency of the ETC at the level downstream of complexes I and II, and improves coupling of ET to OXPHOS. Importantly, to minimize the effect of mitochondrial membrane potential on ET, we used once-frozen mitochondria and demonstrated that SS-20 dose-dependently increases O_2 consumption induced by succinate (Fig. 5E). Finally, the ability of SS-20 to promote respiration after direct reduction of cyt *c* with TMPD (Fig. 5F) without stimulating COX activity (Fig. 5G) identifies cyt *c* as a site of SS-20 activity. We further show that SS-20 does not increase mitochondrial respiration by uncoupling mitochondria as measured by TMRM fluorescence (Fig. 5H). By improving ET at the level of cyt *c*, SS-20 also prevents electron backflow and reduces H_2O_2 production in isolated mitochondria, comparable to that achieved by the uncoupler FCCP (carbonyl cyanide-4-(trifluoromethoxy)phenylhydrazone (Fig. 5I).

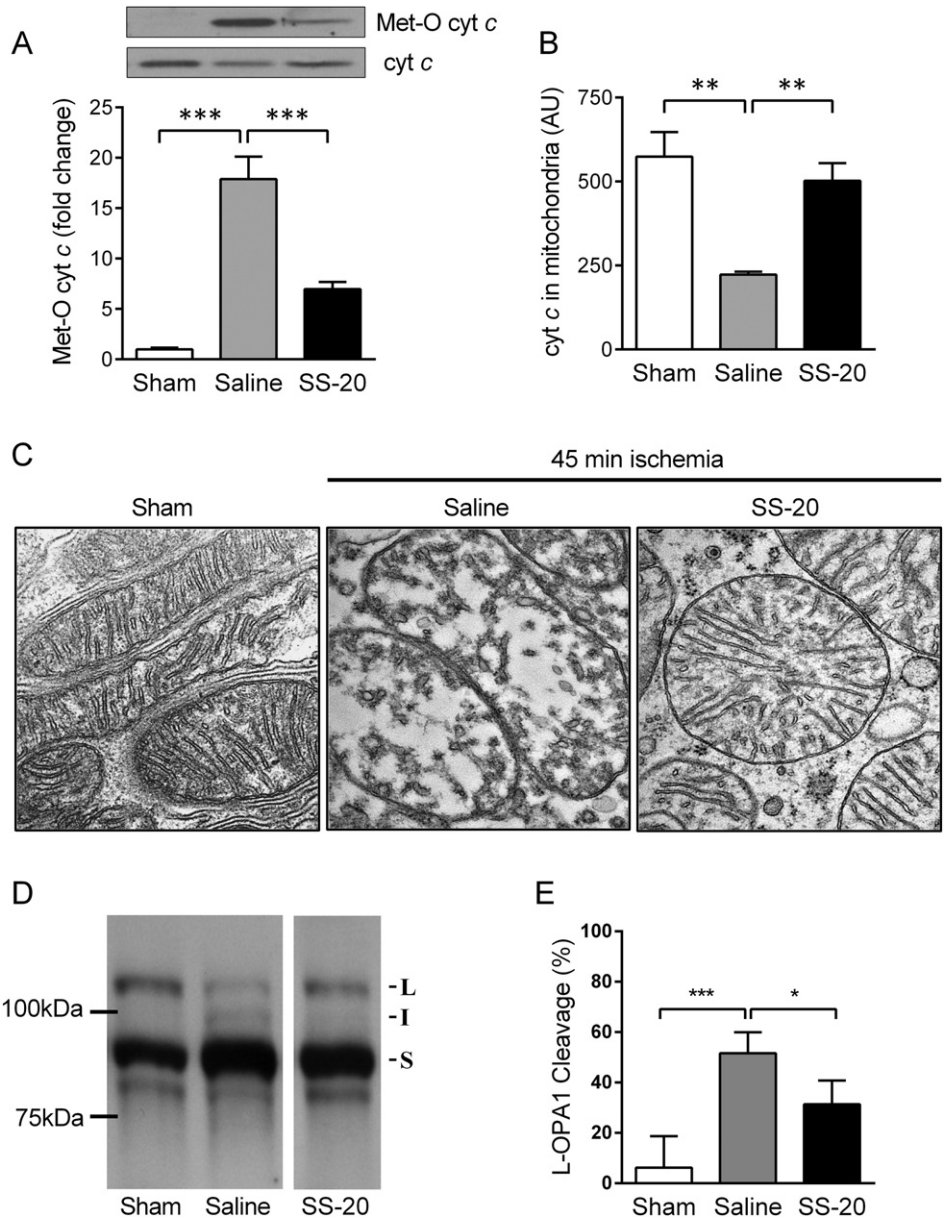

Fig. 2. SS-20 prevents oxidative modification of cyt *c*, cyt *c* release, and cristaeolysis during ischemia. A, Representative western blot and quantification of Met-O cyt *c* formation in mitochondria from rat sham, or ischemic kidneys pre-treated with saline or SS-20. Bands for Met-O cyt *c* and cyt *c* are identified. B, Quantification of cyt *c* in isolated mitochondria from sham or ischemic kidneys of rats, pretreated with saline or SS-20. C, Representative TEM images of mitochondria and cristae morphology under either sham or ischemic conditions pre-treated with saline or SS-20. D–E, Representative western blot (D) and quantification (E) of OPA-1 isoforms from isolated mitochondria. Acute ischemia induces significant cleavage of longest form (L; ~110 kDa) into an intermediate (I; ~95 kDa) form. SS-20 partially prevents this cleavage. Error bars represent SEM (n = 4) **P = 0.01; ***P = 0.001.

4. Discussion

It is now clear that mitochondrial damage incurred during ischemia prevents rapid recovery of ATP upon reperfusion and extends ischemic injury. Ischemia is known to directly inhibit the ETC [8,9], and previous studies suggest that this inhibition is downstream of complex III, either at cyt *c* or complex IV. In this study, we have identified cyt *c* as an early victim of ischemia, and shown that ischemia-induced changes in cyt *c* structure and function account for the inhibition of mitochondrial respiration, cristaeolysis, and cyt *c* release during ischemia (Fig. 6). The reduction in ATP during ischemia promotes hydrophobic interaction between cyt *c* and CL [26,27], resulting in disruption of the Met^{80}-Fe coordination and formation of a globin-like pentacoordinated cyt *c* that is mostly in the ferrous (Fe^{2+}) state during ischemia. This ferrous state of pentacoordinated cyt *c* predisposes the oxidation of Met^{80} to Met^{80}-O [38], and inhibits the re-ligation of Met^{80} to heme Fe [39,40]. The reduction potential of pentacoordinated cyt *c* is significantly lower than native cyt *c*, and this inhibits the reduction of cyt *c* by complex III in the ETC [15,16]. These changes can account for the inhibition of mitochondrial respiration when ischemic mitochondria are exposed to reperfusion conditions. Displacement of Met^{80} from the heme Fe^{2+} converts cyt *c* from an electron carrier to an oxygenase that can oxidize cardiolipin, resulting in cristae degradation and detachment of cyt *c* from the IMM [17–19]. The ultimate release of cyt *c* from the ICS occurs when OPA1 is degraded during ischemia, as OPA1 plays a major role in establishing cristae junctions and keeping the cyt *c* within the ICS [41]. Thus damage to cyt *c* heme structure, together with loss of CL and cyt *c*, explain the slow and incomplete recovery of mitochondrial ATP production upon reperfusion.

SS-20 is a cell-permeable, mitochondria-targeting tetrapeptide that belongs to the Szeto-Schiller (SS) peptides [42,43]. In this study we show that SS-20 can prevent all downstream events caused by the

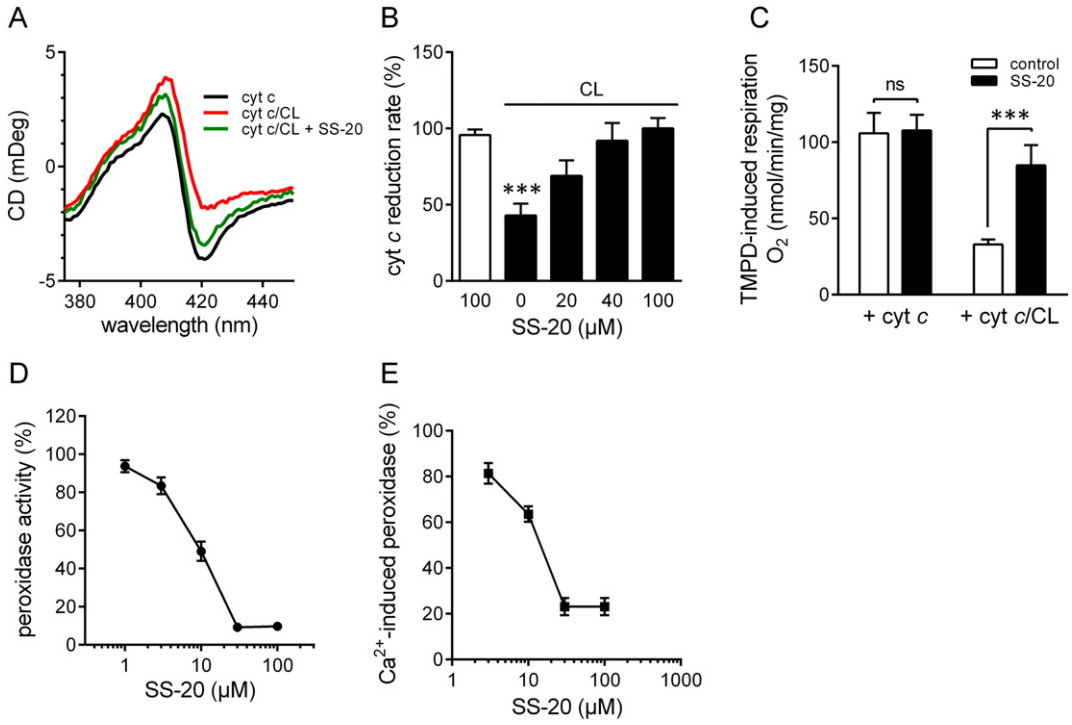

Fig. 3. SS-20 preserves Met^{80}-Fe ligation and protects ET properties of cyt *c* while inhibiting peroxidase activity. A, Circular dichroism was carried out to demonstrate that SS-20 recovered the effect of CL on the negative 418 nm Cotton peak in the Soret spectrum of cyt *c*. B, SS-20 promotes reduction of cyt *c* in the presence of CL. Addition of CL inhibited glutathione-induced cyt *c* reduction by about 60%. SS-20 had no effect on the reduction of cyt *c* in the absence of CL, but dose-dependently rescued the inhibition caused by CL. C, SS-20 promotes oxygen consumption in mitoplasts in the presence of exogenous cyt *c* and excess CL. Mitochondrial respiration was initiated by direct reduction of cyt *c* with TMPD/ascorbate. SS-20 had no effect on O_2 consumption in the presence of added exogenous cyt *c* alone, but restored O_2 consumption inhibited by the addition of CL. D, SS-20 dose-dependently inhibits cyt *c* peroxidase activity induced by CL ($EC_{50} = 9.7 \pm 2.5$ μM). E, SS-20 dose-dependently inhibits cyt *c* peroxidase activity potentiated by Ca^{2+}. Error bars represent SEM (n = 5–9) ***P = 0.001.

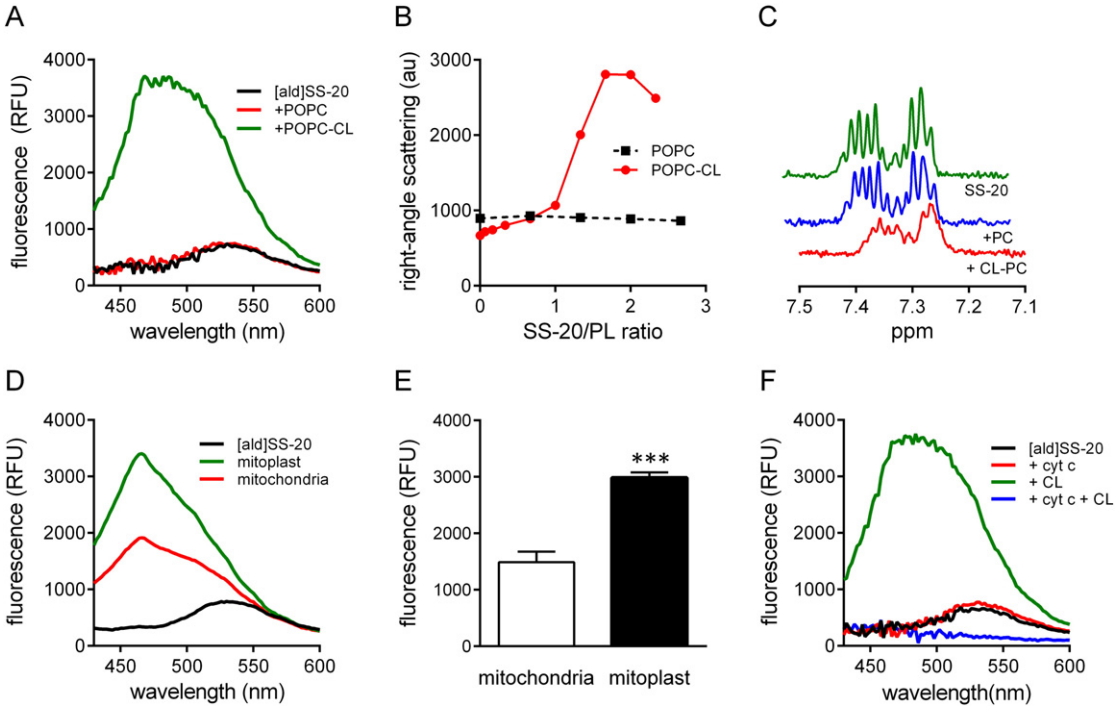

Fig. 4. SS-20 binds selectively to mitochondrial CL and interacts with cyt *c*. A, Representative fluorescence emission spectrum of control [ald]SS-20 and in the presence of POPC liposomes or POPC-CL liposomes. CL-containing liposomes induce blue shift from 535 nm to 465 nm, but POPC liposomes do not. B, SS-20 dose dependently increases light scattering of POPC-CL liposomes, but not POPC liposomes. C, Representative 500 MHz ^{1}H-NMR of the aromatic region (7.5–7.1 ppm). From top, as indicated: (1) SS-20 aromatic protons of phenylalanine (7.4–7.2 ppm); (2) POPC does not substantially affect aromatic proton peaks; (3) CL remodels and broadens the aromatic protons of SS-20. Phospholipids themselves contribute no peaks in this range. D, [ald]SS-20 interacts with both once-frozen mitochondria and *cyt c*-depleted mitoplasts from rat kidney. E, Quantitative analysis of the intensity of the 465 nm peak of [ald]SS-20 in cyt *c*-depleted mitoplasts and once-frozen mitochondria. F, [ald]SS-20 interacts with cyt *c* in the presence of CL. Representative fluorescence emission spectrum of [ald]SS-20 alone, and in the presence of cyt *c*, CL, and a cyt *c* + CL mix. Error bars represent SEM (n = 6) ***P = 0.001.

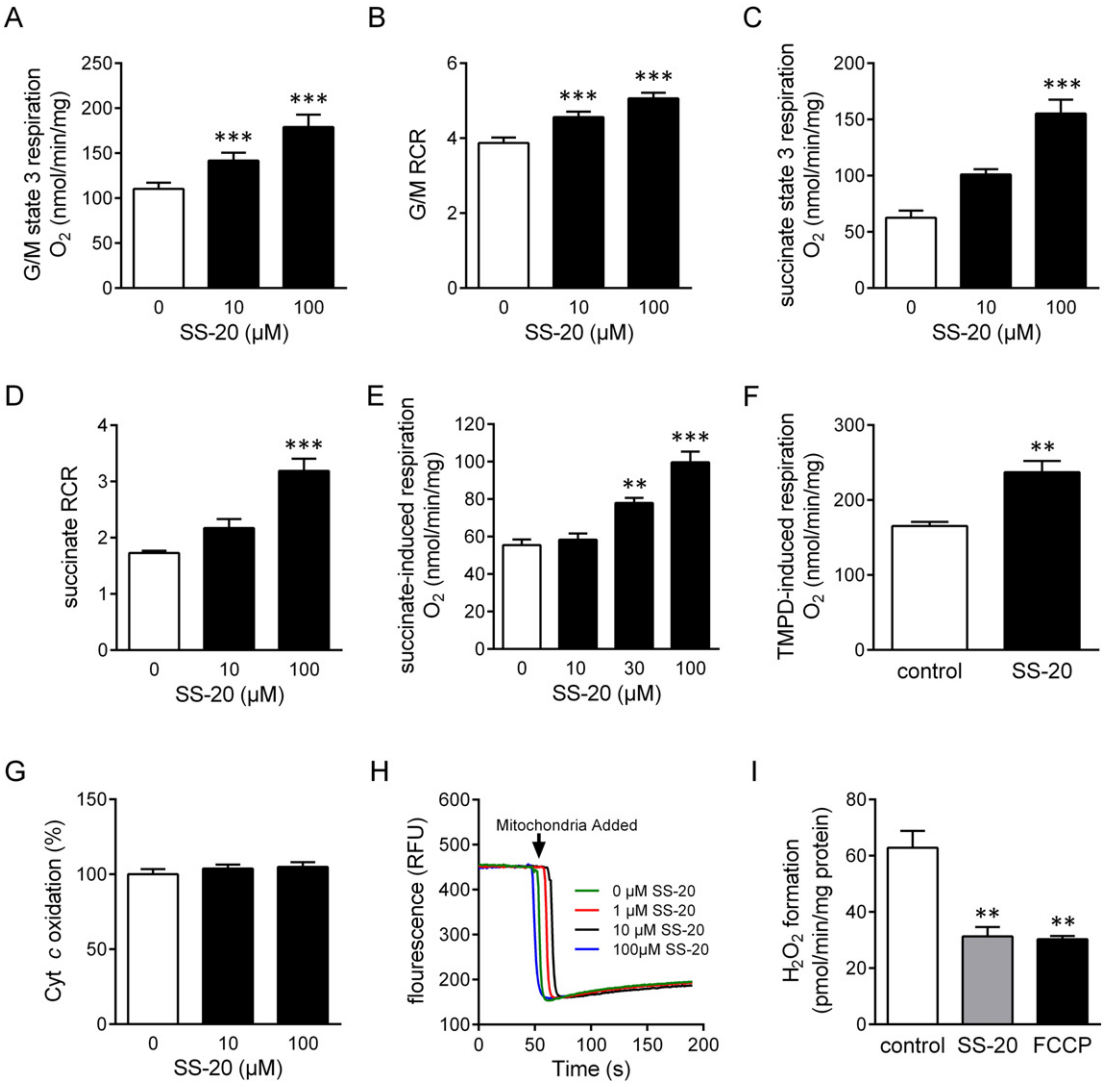

Fig. 5. SS-20 promotes efficiency of ET and inhibits ROS formation in isolated mitochondria. A–B, SS-20 improves glutamate/malate-driven state 3 respiration (A) and RCR (B) in freshly isolated mitochondria. C–D, SS-20 improves succinate-driven state 3 respiration (C) and RCR (D) in freshly isolated mitochondria. E, SS-20 dose-dependently increases O_2 consumption in the presence of succinate in once-frozen mitochondria. F, SS-20 improves O_2 consumption during direct reduction of cyt *c* by TMPD in once-frozen mitochondria. G, SS-20 does not affect COX activity of isolated mitoplasts. H, SS-20 does not affect potential-driven uptake of TMRM into freshly isolated mitochondria. I, Both SS-20 and FCCP reduce the formation of H_2O_2 in isolated mitochondria. Error bars represent SEM (n = 6–7) **P = 0.01; ***P = 0.001.

pentacoordinated heme Fe in cyt *c* (Fig. 6). We provide direct chemical and structural evidence that SS-20 interacts with CL with high selectivity and affinity. In addition, SS-20 interacts with endogenous CL in isolated mitochondria and mitoplasts. Furthermore, our results with the fluorescent analog ([ald]SS-20) indicate that SS-20, when interacting with CL, can penetrate into the heme environment of cyt *c* and protect the Met^{80}-Fe ligation. This is further supported by circular dichroism studies showing that SS-20 protects the negative Cotton peak of cyt *c* against CL-induced damage, thus preserving the stability of the Fe-Met^{80} coordination and π–π interaction within the heme environment [44]. When administered to rats prior to onset of ischemia, SS-20 significantly protected coupled respiration in ischemic mitochondria studied *ex vivo*, including O_2 consumption initiated by direct reduction of cyt *c* with TMPD. These results confirm that ischemia disrupts the heme ligation in cyt *c* and compromises the recovery of mitochondrial ATP synthesis upon reperfusion. Of particular interest is our finding that SS-20 can even increase coupled respiration and reduce H_2O_2 emission in normal mitochondria. It appears that the approach normally used to study isolated mitochondria *ex vivo* actually simulates the condition of ischemic mitochondria upon reperfusion. Isolated mitochondria are relatively depleted of ATP and they are then studied under atmospheric oxygen. In those conditions, even though cyt *c* content is preserved, they are most likely in a hydrophobic interaction with CL and thus exhibit inhibited electron transfer. The SS-20-potentiated oxygen consumption with glutamate/malate (complex I substrates) is similar to those obtained with succinate (complex II substrate), supporting our conclusion that SS-20 stimulates ET downstream of complexes I and II. Furthermore, SS-20 promotes TMPD-induced respiration directly through cyt *c* without affecting COX activity, suggesting that SS-20 optimizes ET through cyt *c*.

Substantial *in vitro* data show that hydrophobic interaction between cyt *c* and CL disrupts the Met^{80}-Fe ligation [32,33,45], but the significance of such hydrophobic interaction *in vivo* has not been demonstrated. Evidence for disruption of the cyt *c* Met^{80}-Fe ligation during ischemia comes from our finding of a 17-fold increase in Met-O cyt *c*. Cyt *c* has two evolutionarily conserved methionine residues (Met^{65} and Met^{80}), but Met^{80} is the preferred site of sulfoxide formation [1,38]. Met-O formation is favored with Fe^{2+} compared to Fe^{3+} cyt *c* [1,38], and cyt *c* is likely to be in the Fe^{2+} state during ischemia as COX is inhibited due to decline in oxygen [46–48]. Interestingly, cyt *c*

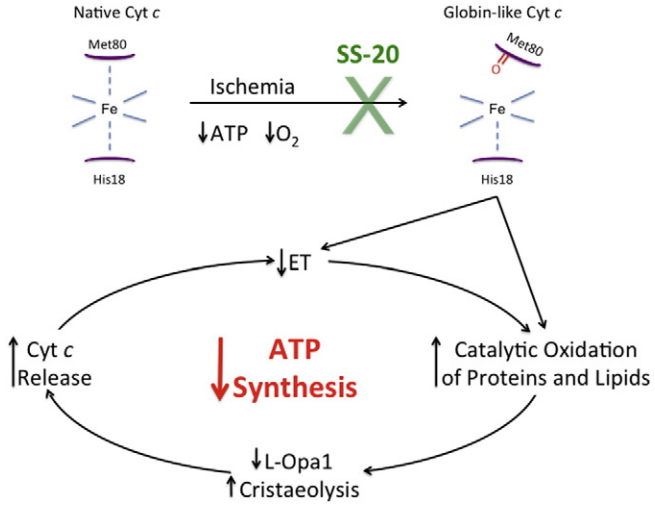

Fig. 6. Schematic diagram illustrating mitochondrial dysfunction in ischemic injury. Decrease in ATP during ischemia promotes hydrophobic interaction of cyt *c* with CL, forming the globin-like pentacoordinated Fe^{2+} cyt *c*. This inhibits ET through cyt *c* and converts this electron carrier into an oxygenase/peroxidase that can oxidize lipids and proteins on the IMM and in the IMS. Oxidation of cardiolipin and proteolytic degradation of OPA1 promote cristaeolysis and cyt *c* release, further diminishing the activity of the mitochondrial ETC and ATP synthesis. SS-20 protects hexacoordination of cyt *c* during ischemia, supports ET through cyt *c*, and prevents oxygenase/peroxidase activity.

Met^{80}-O was detected in the isolated ischemic heart after reperfusion, but the increase was only 2-fold [1]. This much smaller increase in Met-O cyt *c* during reperfusion may correlate with the recovery of COX activity with the re-introduction of O_2.

It was previously thought that excessive matrix ROS is necessary for cyt *c* Met-O formation [1], but it is unclear how matrix ROS can oxidize cyt *c* in the ICS. Interestingly, cyt *c* Met-O formation in isolated mitochondria was induced by inhibition of COX with azide, but not by inhibition of complex III with antimycin [1]. These results would suggest that ROS release is not required since azide did not increase ROS emission [1]. Rather, it would suggest that accumulation of Fe^{2+} cyt *c* is required for Met^{80} oxidation. Furthermore, it should be pointed out that conditions used in *ex vivo* mitochondrial respiration studies (low ATP) promote pentacoordination of cyt *c* [11]. This is consistent with previous findings that self-oxidation of Met^{80} of cyt *c* occurs by its heme and molecular oxygen when Met^{80} dissociates from the heme Fe in a reducing environment [38]. Our results demonstrate that Met-O cyt *c* can be formed during ischemia when there is unlikely to be excessive ROS formation, and it indicates the generation of pentacoordinated Fe^{2+} cyt *c* *in vivo*.

Displacement of Met^{80} from the heme Fe results in opening of the heme crevice and the high spin Fe^{2+} can react with molecular oxygen to form an oxygenase that can oxidize CL without H_2O_2 [17,18]. In addition, the restoration of Fe^{3+} cyt *c* upon reperfusion can be oxidized by H_2O_2 to oxyferryl heme, forming the so-called peroxidase compound I-type intermediate, a highly reactive oxidant that can react with proteins and lipids on the IMM and in the IMS [38,49]. Peroxidase activity and oxidized CL can be readily detected with [cyt *c*/CL] complexes *in vitro* and with isolated mitochondria [18,19]. Cyt *c* oxygenase or peroxidase activity has not been demonstrated *in vivo*, but the presence of Met-O cyt *c* supports the existence of oxygenase/peroxidase activity, which can account for cristae degradation. Degeneration of mitochondrial morphology, especially cristaeolysis, is commonly observed in ischemic mitochondria [3,19,24]. Peroxidized cardiolipin can further elicit a free radical chain reaction even without further ROS production. In addition, peroxidized CL can oxidize Fe^{2+} cyt *c* and cause heme degradation and aggregation [50]. By protecting the heme ligation, SS-20 was able to prevent cristeolysis and maintain mitochondrial cristae architecture during ischemia.

Besides CL, OPA1 localized on the IMM [31,51], is thought to be responsible for cristae assembly, remodeling, and cyt *c* containment within the ICS [41]. Silencing of OPA1 in mammalian cells caused mitochondrial swelling with disintegrated cristae structures [21,52]. Although long (L) and short (S) isoforms of OPA1 are both present on the IMM [23,31,53], depletion of L-OPA1 destabilizes cristae formation, promotes cyt *c* release and inhibits mitochondrial bioenergetics [23,31,53,54]. Importantly, oxidative stress was recently shown to produce sequential cleavage of L-OPA1 to an intermediate OPA1 and later to the S-OPA1 form, resulting in cristae remodeling and release of cyt *c* from the ICS [55,56]. Our study is the first to demonstrate a correlation between oxidative stress in the ICS, degradation of L-OPA1, and loss of mitochondrial cyt *c* *in vivo*. SS-20 was able to inhibit proteolytic degradation of L-OPA1 during ischemia and prevent loss of mitochondrial cyt *c*.

Although ischemia–reperfusion injury is commonly thought to be due to mitochondrial oxidative stress associated with reperfusion, we have identified cyt *c* as an early victim of ischemic injury, and the damage to its heme ligation sets up a feed-forward chain of events that inhibits the mitochondrial ETC and prevents recovery of mitochondrial function upon reperfusion. This has led us to introduce a new therapeutic strategy that emphasizes protection of the heme environment of cyt *c* to optimize electron transfer, minimize ROS production, and prevent the conversion of this electron carrier into a catalytic oxidant.

5. Translational relevance

After the onset of ischemia, timely reperfusion is essential to salvage viable tissue. The ability of reperfusion to restore mitochondrial bioenergetics is dependent on the duration of ischemia, as ischemia causes permanent injury to the mitochondrial ETC. This study has identified cyt *c* as an early victim of ischemia, and the Met^{80}-Fe ligation was specifically demonstrated to be the cause of a cascade of downstream events that limit the recovery of mitochondrial function upon reperfusion. By protecting Met^{80}-Fe ligation in ischemia, SS-20 was able to prevent all downstream mitochondrial injuries and optimize recovery of organ function [2]. SS-20 provides a novel strategy for mitochondrial protection during ischemia and may be beneficial in clinical indications such as elective angioplasty, cardiovascular surgery, partial nephrectomy and transplantation.

Supplementary data to this article can be found online at http://dx.doi.org/10.1016/j.bbabio.2015.06.006.

Conflict of interests

The SS peptides described in this article are licensed for commercial research and development to Stealth Peptides Inc, a clinical stage biopharmaceutical company, in which HHS, AVB and the Cornell Research Foundation have financial interests.

Acknowledgments

This research was supported by the National Institutes of Health (PO1-AG001751), and the Research Program in Mitochondrial Therapeutics at Weill Cornell Medical College. W.E.C. was supported by F31-HL126414 from the National Institutes of Health. We thank Dr. J. David Warren of the Abby and Howard P. Millstein Synthetic Chemistry Core Facility for the synthesis of aladan; Dr. Clay Bracken of the Nuclear Magnetic Resonance Core Facility for assistance with the binding of SS-20 to cardiolipin; and we thank Lee Cohen-Gould and her staff at the Electron Microscopy & Histology Core Facility at Weill Cornell Medical College.

References

[1] V. Borutaite, A. Toleikis, G.C. Brown, In the eye of the storm: mitochondrial damage during heart and brain ischaemia, FEBS J. 280 (2013) 4999–5014.
[2] H.H. Szeto, S. Liu, Y. Soong, A.V. Birk, Improving mitochondrial bioenergetics under ischemic conditions increases warm ischemia tolerance in the kidney, Am. J. Physiol. Ren. Physiol. 308 (2015) F11–F21.
[3] E.J. Lesnefsky, T.I. Gudz, C.T. Migita, M. Ikeda-Saito, M.O. Hassan, P.J. Turkaly, C.L. Hoppel, Ischemic injury to mitochondrial electron transport in the aging heart: damage to the iron–sulfur protein subunit of electron transport complex III, Arch. Biochem. Biophys. 385 (2001) 117–128.
[4] Q. Chen, S. Moghaddas, C.L. Hoppel, E.J. Lesnefsky, Ischemic defects in the electron transport chain increase the production of reactive oxygen species from isolated rat heart mitochondria, Am. J. Physiol. Cell Physiol. 294 (2008) C460–C466.
[5] Q. Chen, G. Yin, S. Stewart, Y. Hu, E.J. Lesnefsky, Isolating the segment of the mitochondrial electron transport chain responsible for mitochondrial damage during cardiac ischemia, Biochem. Biophys. Res. Commun. 397 (2010) 656–660.
[6] E.J. Lesnefsky, B. Tandler, J. Ye, T.J. Slabe, J. Turkaly, C.L. Hoppel, Myocardial ischemia decreases oxidative phosphorylation through cytochrome oxidase in subsarcolemmal mitochondria, Am. J. Physiol. 273 (1997) H1544–H1554.
[7] E.J. Lesnefsky, Q. Chen, T.J. Slabe, M.S. Stoll, P.E. Minkler, M.O. Hassan, B. Tandler, C.L. Hoppel, Ischemia, rather than reperfusion, inhibits respiration through cytochrome oxidase in the isolated, perfused rabbit heart: role of cardiolipin, Am. J. Physiol. Heart Circ. Physiol. 287 (2004) H258–H267.
[8] Q. Chen, E.J. Lesnefsky, Depletion of cardiolipin and cytochrome c during ischemia increases hydrogen peroxide production from the electron transport chain, Free Radic. Biol. Med. 40 (2006) 976–982.
[9] E. Gnaiger, A.V. Kuznetsov, Mitochondrial respiration at low levels of oxygen and cytochrome c, Biochem. Soc. Trans. 30 (2002) 252–258.
[10] G. De Sanctis, C. Ciaccio, G.F. Fasciglione, L. Fiorucci, M. Gioia, F. Sinibaldi, S. Marini, R. Santucci, M. Coletta, Effect of axial coordination on the kinetics of assembly and folding of the two halves of horse heart cytochrome C, J. Biol. Chem. 279 (2004) 52860–52868.
[11] T.M. Josephs, M.D. Liptak, G. Hughes, A. Lo, R.M. Smith, S.M. Wilbanks, K.L. Bren, E.C. Ledgerwood, Conformational change and human cytochrome c function: mutation of residue 41 modulates caspase activation and destabilizes Met-80 coordination, J. Biol. Inorg. Chem. 18 (2013) 289–297.
[12] S. Zaidi, M.I. Hassan, A. Islam, F. Ahmad, The role of key residues in structure, function, and stability of cytochrome-c, Cell. Mol. Life Sci. 71 (2013) 229–255.
[13] A.V. Birk, W.M. Chao, C. Bracken, J.D. Warren, H.H. Szeto, Targeting mitochondrial cardiolipin and the cytochrome c/cardiolipin complex to promote electron transport and optimize mitochondrial ATP synthesis, Br. J. Pharmacol. 171 (2014) 2017–2028.
[14] F. Sinibaldi, E. Droghetti, F. Polticelli, M.C. Piro, D. Di Pierro, T. Ferri, G. Smulevich, R. Santucci, The effects of ATP and sodium chloride on the cytochrome c-cardiolipin interaction: the contrasting behavior of the horse heart and yeast proteins, J. Inorg. Biochem. 105 (2011) 1365–1372.
[15] E.J. Snider, J. Muenzner, J.R. Toffey, Y. Hong, E.V. Pletneva, Multifaceted effects of ATP on cardiolipin-bound cytochrome c, Biochemistry 52 (2013) 993–995.
[16] J. Muenzner, J.R. Toffey, Y. Hong, E.V. Pletneva, Becoming a peroxidase: cardiolipin-induced unfolding of cytochrome c, J. Phys. Chem. B 117 (2013) 12878–12886.
[17] F. Sinibaldi, B.D. Howes, M.C. Piro, F. Polticelli, C. Bombelli, T. Ferri, M. Coletta, G. Smulevich, R. Santucci, Extended cardiolipin anchorage to cytochrome c: a model for protein-mitochondrial membrane binding, J. Biol. Inorg. Chem. 15 (2010) 689–700.
[18] E.K. Tuominen, C.J. Wallace, P.K. Kinnunen, Phospholipid–cytochrome c interaction: evidence for the extended lipid anchorage, J. Biol. Chem. 277 (2002) 8822–8826.
[19] Z. Wang, Y. Ando, A.D. Nugraheni, C. Ren, S. Nagao, S. Hirota, Self-oxidation of cytochrome c at methionine80 with molecular oxygen induced by cleavage of the Met-heme iron bond, Mol. BioSyst. 10 (2014) 3130–3137.
[20] Z. Salamon, G. Tollin, Interaction of horse heart cytochrome c with lipid bilayer membranes: effects on redox potentials, J. Bioenerg. Biomembr. 29 (1997) 211–221.
[21] L.V. Basova, I.V. Kurnikov, L. Wang, V.B. Ritov, N.A. Belikova, I.I. Vlasova, A.A. Pacheco, D.E. Winnica, J. Peterson, H. Bayir, D.H. Waldeck, V.E. Kagan, Cardiolipin switch in mitochondria: shutting off the reduction of cytochrome c and turning on the peroxidase activity, Biochemistry 46 (2007) 3423–3434.
[22] J.M. Bradley, G. Silkstone, M.T. Wilson, M.R. Cheesman, J.N. Butt, Probing a complex of cytochrome c and cardiolipin by magnetic circular dichroism spectroscopy: implications for the initial events in apoptosis, J. Am. Chem. Soc. 133 (2011) 19676–19679.
[23] V.E. Kagan, V.A. Tyurin, J. Jiang, Y.Y. Tyurina, V.B. Ritov, A.A. Amoscato, A.N. Osipov, N.A. Belikova, A.A. Kapralov, V. Kini, I.I. Vlasova, Q. Zhao, M. Zou, P. Di, D.A. Svistunenko, I.V. Kurnikov, G.G. Borisenko, Cytochrome c acts as a cardiolipin oxygenase required for release of proapoptotic factors, Nat. Chem. Biol. 1 (2005) 223–232.
[24] H.S. Aluri, D.C. Simpson, J.C. Allegood, Y. Hu, K. Szczepanek, S. Gronert, Q. Chen, E.J. Lesnefsky, Electron flow into cytochrome c coupled with reactive oxygen species from the electron transport chain converts cytochrome c to a cardiolipin peroxidase: role during ischemia–reperfusion, Biochim. Biophys. Acta 1840 (2014) 3199–3207.
[25] H.H. Szeto, S. Liu, Y. Soong, D. Wu, S.F. Darrah, F.Y. Cheng, Z. Zhao, M. Ganger, C.Y. Tow, S.V. Seshan, Mitochondria-targeted peptide accelerates ATP recovery and reduces ischemic kidney injury, J. Am. Soc. Nephrol. 22 (2011) 1041–1052.
[26] A.V. Birk, S. Liu, Y. Soong, W. Mills, P. Singh, J.D. Warren, S.V. Seshan, J.D. Pardee, H.H. Szeto, The mitochondrial-targeted compound SS-31 re-energizes ischemic mitochondria by interacting with cardiolipin, J. Am. Soc. Nephrol. 24 (2013) 1250–1261.
[27] K. Zhao, G.M. Zhao, D. Wu, Y. Soong, A.V. Birk, P.W. Schiller, H.H. Szeto, Cell-permeable peptide antioxidants targeted to inner mitochondrial membrane inhibit mitochondrial swelling, oxidative cell death, and reperfusion injury, J. Biol. Chem. 279 (2004) 34682–34690.
[28] H.H. Szeto, Mitochondria-targeted cytoprotective peptides for ischemia–reperfusion injury, Antioxid. Redox Signal. 10 (2008) 601–619.
[29] A. Olichon, L. Baricault, N. Gas, E. Guillou, A. Valette, P. Belenguer, G. Lenaers, Loss of OPA1 perturbates the mitochondrial inner membrane structure and integrity, leading to cytochrome c release and apoptosis, J. Biol. Chem. 278 (2003) 7743–7746.
[30] S. Cipolat, O. Martins de Brito, B. Dal Zilio, L. Scorrano, OPA1 requires mitofusin 1 to promote mitochondrial fusion, Proc. Natl. Acad. Sci. U. S. A. 101 (2004) 15927–15932.
[31] L. Griparic, T. Kanazawa, A.M. van der Bliek, Regulation of the mitochondrial dynamin-like protein Opa1 by proteolytic cleavage, J. Cell Biol. 178 (2007) 757–764.
[32] R.C. Scaduto Jr., L.W. Grotyohann, Measurement of mitochondrial membrane potential using fluorescent rhodamine derivatives, Biophys. J. 76 (1999) 469–477.
[33] H.H. Szeto, P.W. Schiller, K. Zhao, G. Luo, Fluorescent dyes alter intracellular targeting and function of cell-penetrating tetrapeptides, FASEB J. 19 (2005) 118–120.
[34] R.S. Prosser, F. Evanics, J.L. Kitevski, M.S. Al-Abdul-Wahid, Current applications of bicelles in NMR studies of membrane-associated amphiphiles and proteins, Biochemistry 45 (2006) 8453–8465.
[35] G. Wirthensohn, W.G. Guder, Renal substrate metabolism, Physiol. Rev. 66 (1986) 469–497.
[36] K.L. Klein, M.S. Wang, S. Torikai, W.D. Davidson, K. Kurokawa, Substrate oxidation by isolated single nephron segments of the rat, Kidney Int. 20 (1981) 29–35.
[37] S. Uchida, H. Endou, Substrate specificity to maintain cellular ATP along the mouse nephron, Am. J. Physiol. 255 (1988) F977–F983.
[38] N. Ishihara, Y. Fujita, T. Oka, K. Mihara, Regulation of mitochondrial morphology through proteolytic cleavage of OPA1, EMBO J. 25 (2006) 2966–2977.
[39] J.B. Soffer, E. Fradkin, L.A. Pandiscia, R. Schweitzer-Stenner, The (not completely irreversible) population of a misfolded state of cytochrome c under folding conditions, Biochemistry 52 (2013) 1397–1408.
[40] Y.A. Vladimirov, E.V. Proskurnina, D.Y. Izmailov, A.A. Novikov, A.V. Brusnichkin, A.N. Osipov, V.E. Kagan, Mechanism of activation of cytochrome C peroxidase activity by cardiolipin, Biochemistry (Mosc) 71 (2006) 989–997.
[41] R. Santucci, F. Ascoli, The Soret circular dichroism spectrum as a probe for the heme Fe(III)–Met(80) axial bond in horse cytochrome c, J. Inorg. Biochem. 68 (1997) 211–214.
[42] B.E. Cohen, T.B. McAnaney, E.S. Park, Y.N. Jan, S.G. Boxer, L.Y. Jan, Probing protein electrostatics with a synthetic fluorescent amino acid, Science 296 (2002) 1700–1703.
[43] Y.P. Myer, S. Kumar, Methionine-oxidized horse heart cytochrome c. III. Ascorbate reduction and the methionine-80-sulfur-iron linkage, J. Protein Chem. 8 (1989) 33–50.
[44] J. Pande, K. Kinnally, K.K. Thallum, B.C. Verma, Y.P. Myer, L. Rechsteiner, H.R. Bosshard, Methionine-oxidized horse heart cytochrome c. I. Reaction with chloramine-T, products, and their oxidoreduction properties, J. Protein Chem. 6 (1987) 295–319.
[45] C. Frezza, S. Cipolat, O. Martins de Brito, M. Micaroni, G.V. Beznoussenko, T. Rudka, D. Bartoli, R.S. Polishuck, N.N. Danial, B. De Strooper, L. Scorrano, OPA1 controls apoptotic cristae remodeling independently from mitochondrial fusion, Cell 126 (2006) 177–189.
[46] M.C. Hsu, R.W. Woody, The origin of the heme Cotton effects in myoglobin and hemoglobin, J. Am. Chem. Soc. 93 (1971) 3515–3525.
[47] N.A. Brazhe, M. Treiman, B. Faricelli, J.H. Vestergaard, O. Sosnovtseva, In situ Raman study of redox state changes of mitochondrial cytochromes in a perfused rat heart, PLoS One 8 (2013) e70488.
[48] D.F. Wilson, W.L. Rumsey, T.J. Green, J.M. Vanderkooi, The oxygen dependence of mitochondrial oxidative phosphorylation measured by a new optical method for measuring oxygen concentration, J. Biol. Chem. 263 (1988) 2712–2718.
[49] A. Pohlmann, K. Cantow, J. Hentschel, K. Arakelyan, M. Ladwig, B. Flemming, U. Hoff, P.B. Persson, E. Seeliger, T. Niendorf, Linking non-invasive parametric MRI with invasive physiological measurements (MR-PHYSIOL): towards a hybrid and integrated approach for investigation of acute kidney injury in rats, Acta Physiol. (Oxf.) 207 (2013) 673–689.
[50] A. Lawrence, C.M. Jones, P. Wardman, M.J. Burkitt, Evidence for the role of a peroxidase compound I-type intermediate in the oxidation of glutathione, NADH, ascorbate, and dichlorofluorescin by cytochrome c/H_2O_2. Implications for oxidative stress during apoptosis, J. Biol. Chem. 278 (2003) 29410–29419.
[51] A. Musatov, M. Fabian, R. Varhac, Elucidating the mechanism of ferrocytochrome c heme disruption by peroxidized cardiolipin, J. Biol. Inorg. Chem. 18 (2012) 137–144.
[52] A. Olichon, L.J. Emorine, E. Descoins, L. Pelloquin, L. Brichese, N. Gas, E. Guillou, C. Delettre, A. Valette, C.P. Hamel, B. Ducommun, G. Lenaers, P. Belenguer, The human dynamin-related protein OPA1 is anchored to the mitochondrial inner membrane facing the inter-membrane space, FEBS Lett. 523 (2002) 171–176.
[53] L. Griparic, N.N. van der Wel, I.J. Orozco, P.J. Peters, A.M. van der Bliek, Loss of the intermembrane space protein Mgm1/OPA1 induces swelling and localized constrictions along the lengths of mitochondria, J. Biol. Chem. 279 (2004) 18792–18798.
[54] Z. Song, H. Chen, M. Fiket, C. Alexander, D.C. Chan, OPA1 processing controls mitochondrial fusion and is regulated by mRNA splicing, membrane potential, and Yme1L, J. Cell Biol. 178 (2007) 749–755.
[55] S. Cipolat, T. Rudka, D. Hartmann, V. Costa, L. Serneels, K. Craessaerts, K. Metzger, C. Frezza, W. Annaert, L. D'Adamio, C. Derks, T. Dejaegere, L. Pellegrini, R. D'Hooge, L. Scorrano, B. De Strooper, Mitochondrial rhomboid PARL regulates cytochrome c release during apoptosis via OPA1-dependent cristae remodeling, Cell 126 (2006) 163–175.
[56] X. Wang, H. Li, A. Zheng, L. Yang, J. Liu, C. Chen, Y. Tang, X. Zou, Y. Li, J. Long, Y. Zhang, Z. Feng, Mitochondrial dysfunction-associated OPA1 cleavage contributes to muscle degeneration: preventative effect of hydroxytyrosol acetate, Cell Death Dis. 5 (2014) e1521.